

OUTER ATMOSPHERES OF COOL STARS. IX. A SURVEY OF ULTRAVIOLET EMISSION FROM F–K DWARFS AND GIANTS WITH *IUE*

THOMAS R. AYRES,^{1,2} NORMAN C. MARSTAD AND JEFFREY L. LINSKY^{2,3}
 Joint Institute for Laboratory Astrophysics, University of Colorado and National Bureau of Standards
 Received 1980 September 5; accepted 1981 January 26

ABSTRACT

We report preliminary results of an ultraviolet survey of cool-star emission properties with *IUE*. We present 1150–2000 Å spectra of representative F–K dwarfs and giants and construct correlation diagrams that compare chromospheric ($T \lesssim 10^4$ K) and transition-region ($T \approx 10^5$ K) emission line strengths, and broad-band coronal ($T \gtrsim 10^6$ K) soft-X-ray fluxes. We find that the transition-region (TR) and coronal emission in the G–K dwarfs and G giants is well correlated with the Mg II $\lambda 2800$ doublet emission strength, which in turn is symptomatic of chromospheric energy losses. However, the power-law slopes are steeper than unity, particularly for soft X-rays. We conclude that while the distinct atmospheric layers very likely are physically associated, the internal heating mechanisms must be quite different. Despite the apparent chromosphere-TR-corona correlations among the G–K dwarfs and G giants, the earlier (F) and later (K) giants exhibit anomalous behavior. The former appear to have brighter TRs for a given chromospheric emission level, while the latter are systematically deficient in $T \gtrsim 10^5$ K material. In fact, not only are TRs very weak among the red giants, but chromospheres and coronae are systematically weak as well (at least compared with the mean activity levels of F–G giants). We propose that the weakness of hot outer atmospheres in the red giants compared with the yellow giants can be understood as a consequence of stellar evolution since stars of slightly different spectral type in the giant branch likely have very different main-sequence progenitors.

Subject headings: stars: chromospheres — stars: coronae — stars: emission-line — stars: late-type — ultraviolet: spectra

I. INTRODUCTION

During the past several years a revolution has occurred in our ability to study physical conditions in the outer layers of stellar atmospheres analogous to the solar chromosphere and corona. The *International Ultraviolet Explorer* (*IUE*; Boggess *et al.* 1978) now permits the routine study of cool-star spectra in the $\lambda 1150$ –3000 region of even faint stars (Linsky *et al.* 1978), whereas previously only a handful of the brightest late-type stars had been detected by *Copernicus* (Dupree 1975) or rocket (Vitz *et al.* 1976) and balloon spectrometers (e.g., Kondo, Morgan, and Modisette 1976). Furthermore, the hot ($\sim 10^6$ K) coronal layers of the stellar outer atmosphere are now readily detected in stars populating most regions of the Hertzsprung-Russell (H-R) diagram by the sensitive soft-X-ray imaging instruments on the *Einstein* Observatory (Vaiana *et al.* 1980). Previously only the bright coronae of RS CVn-type binary systems (Walter,

Charles, and Bowyer 1978) and a few nearby stars (Cash *et al.* 1978; Nugent and Garmire 1978; Ayres *et al.* 1979; Cash *et al.* 1979; Walter *et al.* 1980b) had been seen in the *HEAO 1* all-sky survey or earlier satellite and sounding rocket flights (Mewe *et al.* 1975; Topka *et al.* 1979, and references to previous work therein). At the same time, detailed reconnaissance of the solar chromosphere-corona by imaging and spectroscopic instruments on *Skylab*, and subsequent high-resolution spectroscopy by *OSO 8* and the *Solar Maximum Mission* experiments, have provided essential insight concerning the physical structure and heating of the solar outer atmosphere.

The time is ripe, therefore, to examine the growing body of stellar ultraviolet spectra obtained with *IUE*, and to try to identify connections between the gross properties of cool-star outer atmospheres and the detailed picture of the solar chromosphere-corona that has emerged over the past decade. We present our survey in the form of a progress report. Our study is by no means complete: Only a limited number of spectra have been analyzed fully and many stars remain to be observed. However, enough information has accumulated that we can begin to draw some useful conclusions.

¹Now at the Laboratory for Atmospheric and Space Physics, University of Colorado.

²Guest Observer with the *International Ultraviolet Explorer* (*IUE*) satellite.

³Staff Member, Quantum Physics Division, National Bureau of Standards, Boulder, Colorado.

Our report is divided as follows: In § II, we present low-dispersion ultraviolet spectra (λ 1150–2000) of a representative sample of cool stars, including dwarfs and giants of spectral types F–K. We describe how the observations were taken, how an absolute calibration was applied, and what information can be extracted from such spectra. In § III, we present our data and other published line strengths as correlation diagrams that compare chromospheric and transition-region line strengths and coronal soft-X-ray fluxes as a function of the emission intensity of the chromospheric Mg II λ 2800 doublet. In § IV we discuss implications of the apparent correlations with respect to the weakening or disappearance of transition regions and hot coronae in the cool half of the red-giant branch (Linsky and Haisch 1979), and possible chromospheric and coronal heating mechanisms. Finally, we propose a speculative scenario to explain why the yellow giants tend to have active chromospheres and coronae, while the red giants tend to be comparatively inactive.

II. IUE SHORT-WAVELENGTH SPECTRA OF SELECTED COOL STARS

The spectra described here were obtained through several guest observing programs with IUE. Pertinent information concerning the individual exposures is summarized in Table 1.

All of the targets, with the exception of Procyon and Arcturus, were observed through the large aperture ($10'' \times 20''$). The low-dispersion images were examined carefully for particle radiation "hits," reseau marks, and other blemishes. Where possible, spurious emission spikes were removed from the extracted spectra. The background-corrected net spectra were then multiplied by the Bohlin *et al.* (1980) inverse sensitivity curve for the SWP camera (spectral bandpass 1150–2000 Å) and divided by the exposure time. The small-aperture Procyon spectra were placed on an absolute scale by comparing the apparent fluxes of prominent emission lines with the large-aperture results published by Brown and Jordan (1980*a*). (The normalization is equivalent to an effective 30% transmission for the small slot.) A similar approach was applied to Arcturus (see below). All of the spectra presented here have been corrected to the revised intensity transfer function (ITF) according to the algorithm proposed by Holm (1979; see also Cassatella *et al.* 1980).

a) Low-Dispersion Spectra

Sample spectra are presented in Figures 1–3. The ordinates of the diagrams are normalized fluxes; that is, the absolute monochromatic flux measured at the Earth f_{λ} (ergs $\text{cm}^{-2} \text{s}^{-1} \text{Å}^{-1}$) divided by the stellar bolometric luminosity l_{bol} (ergs $\text{cm}^{-2} \text{s}^{-1}$), also measured at the Earth. The resulting fluxes have units of Å^{-1} and repre-

TABLE 1
SUMMARY OF IUE OBSERVATIONS

Star	Bright Star Catalog	Spectral Type	Date	IUE Exposure Number (SWP)	Exposure Time (minutes)
ξ Boo A ^a ...	5544	G8 V	1978 Aug 21	2347	90
ε Eri	1084	K2 V	1978 Aug 23	2376	60
β Cas	21	F2 IV	1978 Aug 23	2373	6.5
			1978 Aug 23	2372	26
α CMi	2943	F5 IV–V	1978 Apr 6	1318 ^b	6
			1978 Apr 6	1319 ^b	10
			1978 Apr 6	1320 ^b	20
			1978 Apr 3	1306 ^b	30
γ Boo	5435	A7 III	1978 Aug 25	2395	24
μ Vel	4216	G5 III	1978 Aug 19	2338	15
			1978 Aug 23	2377	4
λ And	8961	G8 III–IV+	1978 Aug 26	2399	32
			1978 Aug 26	2400	60
β Cet	188	K1 III	1978 Aug 23	2371	40
ε Sco	6241	K2 III–IV	1978 Aug 26	2401	80
α Ser	5854	K2 III	1978 Aug 23	2378	50
			1978 Aug 25	2397	101
α Boo	5340	K2 III	1978 Apr 6	1315 ^b	20
			1978 Apr 6	1316 ^b	240
α UMa	4301	K0 II–III+	1978 Aug 25	2396	50
α Car	2326	F0 Ib–II	1979 Jun 7	5439	60

^aξ Boo B is present but very weak in this spectrum.

^bSmall-aperture (3" diameter) spectrum.

sent the monochromatic fraction of the stellar bolometric output at a particular wavelength. (The apparent fluxes at the Earth can be recovered by multiplying the normalized fluxes by l_{bol} , which is listed in the fifth column of the table.)

The flux ratios are a fair way to compare stars of very different surface areas, dwarfs and giants for example. Furthermore, the flux ratios are independent of uncertain stellar distances, although they are somewhat sensitive to bolometric corrections. The normalized fluxes are analogous to surface fluxes presented in previous papers of this series, and the sum for all emissions formed in a given atmospheric layer is an empirical measure of the radiative cooling of that layer (which must be balanced by a heat input at least as large). Surface fluxes, which are useful for atmospheric modeling, may be derived straightforwardly from the apparent fluxes and stellar angular diameters listed in Table 2.

The defining relation we adopt for l_{bol} is,

$$l_{\text{bol}} = 2.7 \times 10^{-5} \times 10^{-m_{\text{bol}}/2.5} \text{ ergs cm}^{-2} \text{ s}^{-1} \quad (1)$$

at the Earth, where

$$m_{\text{bol}} = V + \text{B.C.}$$

The proportionality constant is appropriate to the solar apparent visual magnitude $V_{\odot} = -26.76$ mag (Flannery and Ayres 1978), the apparent solar bolometric luminosity $l_{\odot} = 1.37 \times 10^6 \text{ ergs cm}^{-2} \text{ s}^{-1}$ (Fröhlich 1977), and an adopted bolometric correction $\text{B.C.}_{\odot} \equiv 0$. Stellar bolometric corrections were established relative to $\text{B.C.}_{\odot} = 0$ using the $\text{B.C.} - (V - R)$ relations for dwarfs, giants, and supergiants proposed by Johnson (1966). Apparent visual magnitudes and $(V - R)$ colors were taken from Johnson *et al.* (1966).

In Figure 1 we compare the SWP spectrum of the late-A giant γ Boo with those of the F subgiants β Cas and Procyon (α CMi). A-type stars are commonly presumed not to possess chromospheres and transition regions, because the convective motions thought necessary to sustain the hot outer atmosphere are very weak or absent entirely in such stars (Böhm-Vitense and Dettmann 1980). However, F-type stars have convective envelopes and are expected to possess solar-like chromospheres and transition regions.

The spectrum of γ Boo shows no evidence for the chromospheric (e.g., O I $\lambda 1305$) or transition-region emission features (C II $\lambda 1335$, C IV $\lambda 1550$) that are prominent in the F-star spectra (and in the solar ultraviolet spectrum). (Note, the $\lambda 1216$ L α "emission" in the γ Boo spectrum is entirely *geocoronal* and the emission spikes appearing near $\lambda 1320$ and $\lambda 1410$ very likely are gaps between photospheric absorption lines.) However, the very bright *photospheric* spectrum of γ Boo, with its unresolved absorption line structure, provides a difficult

background against which to search for weak chromospheric or transition-region emission features. (Note: part of the "photospheric" emission in the short-wavelength region is scattered light from longer wavelengths.) In fact, emission lines with surface fluxes as large as those of β Cas probably would not be detectable against the bright photospheric spectrum of γ Boo (Linsky and Marstad 1980). Consequently, the *IUE* short-wavelength region is poorly suited to search for hot outer atmospheres in A-type and earlier stars. Instead, one must observe the extreme ultraviolet and soft-X-ray regions where the photospheric emission is weak and the contrast of features formed at $T \gtrsim 10^5$ K is enhanced. Indeed, some A-type stars have been detected as weak soft-X-ray sources by *Einstein* (Vaiana *et al.* 1980; Cash and Snow 1980) and previous experiments (Topka *et al.* 1979; Cash, Snow, and Charles 1979).

Chromospheric and transition-region emission lines are seen clearly in the F-star spectra, and we conclude that chromospheres and transition regions are a common phenomenon among such stars (see also Böhm-Vitense and Dettmann 1980). Coronae likely also are common: the *Einstein* stellar survey team has reported that F stars as a class are strong soft-X-ray emitters (Vaiana *et al.* 1980).

Figure 2 extends the ultraviolet spectral comparison to G–K dwarfs, including the Sun. The solar spectrum depicted in the top panel is a photometrically precise rocket irradiance spectrum (Mount, Rottman, and Timothy 1980) that has been degraded to the 6 Å FWHM resolution of the *IUE* low-dispersion mode. The measurement was obtained on 1979 June 5 during a moderately active phase of the sunspot cycle. The ultraviolet line fluxes cited here are typically twice those of the analogous quiet Sun (i.e., sunspot minimum) spectrum illustrated in previous papers of this series (e.g., Ayres and Linsky 1980*a, b*).

The middle and bottom panels of Figure 2 demonstrate that the cool dwarf stars ξ Boo A and ϵ Eri have brighter emission-line spectra (in $f_{\lambda}/l_{\text{bol}}$ units) than even the moderately active Sun.⁴ All of the solar-like chromospheric and transition-region emission features are present, including N V $\lambda 1240$, O I $\lambda 1305$, C II $\lambda 1335$, Si IV $\lambda \lambda 1394, 1403$, C IV $\lambda 1550$, He II $\lambda 1640$, and Si II $\lambda \lambda 1808, 1816$. However, the normalized line strengths of the two active dwarfs are up to an order of magnitude larger than the solar counterparts.

Note also that the photospheric continuum emission in the $\lambda > 1600$ Å region falls dramatically from early G

⁴Observations of ξ Boo A and ϵ Eri have been reported previously by Hartmann *et al.* (1979) and by Linsky *et al.* (1978). Here, we present optimally exposed spectra of both stars that have been corrected for the ITF error (see above). Our SWP spectrum of ϵ Eri supersedes the early spectrum described by Linsky *et al.*, which was reduced with an incorrect dispersion constant and only a preliminary absolute calibration.

TABLE 2
EMISSION LINE FLUX RATIOS

STAR	SPECTRAL TYPE	$V-R$	ϕ^a (10^{-3} arcsec)	I_{bol} (10^{-7} ergs $\text{cm}^{-2} \text{s}^{-1}$)	f_i/I_{bol} (10^{-7})										Soft X-rays	Ref. ^b
					Mg II 2800	O I 1305	Si II 1815	C II 1335	He II 1640	N V 1240	Si IV 1400	C IV 1550	Σ Lines	10^5K		
Sun	G2 V ^{sp,max} _{sp,min}	0.53:	...	1.37×10^{13}	280	1.6	3.1	2.4	0.8	0.14	1.1	2.1	3.3	4	1	
α Cen	F2 V	0.34	0.775	4.1	200	0.7	3.5	0.8	0.2	0.06	0.4	0.9	1.3	1.5	2	
α Cen A	G2 V	0.53:	8.79	270	180	1.0	4.5:	1.0	0.3	0.3:	0.6	1.0	1.8	2	3,4	
ξ Boo A	G8 V	0.63	1.32	5.3	770	6.5	23	8.6	8.8	4.0	8.1	15	27	530	1,5,6	
α Cen B	K1 V	0.67:	6.26	95	250	1.4	5.2	1.3	0.2	0.2:	0.9	1.2	2.2	14	3,4	
ϵ Eri	K2 V	0.73	2.29	10.3	750	5.3	19	6.7	5.3	1.8	4.1	9.8	16	150	1,6,7	
β Cas	F2 IV	0.31	2.01	30	230	7.7	...	6.7	...	1.5	5.3	16	23	...	1	
μ Vir	F3 IV	0.40	1.13	7.1	150	16	7.5	15	23	...	2	
ι Leo	F3 IV	0.39	1.09	6.8	290	8.2	...	14	9.3	30	30	...	2	
α CMi	F5 IV-V	0.42	6.02	180	160:	1.6	...	3.2	...	0.6:	1.8:	4.8	7.2	...	1,8	
UX Ari	G5 V+K0 IV	0.54:	0.427	0.93	3000	106	87	110	120	...	60	160	270	7500	9,10	
HR 1099	G5 IV+K0 IV	0.54	0.561	1.44	4200	76	110	130	100	47	67	220	330	6000	9,10	
α Aur Ab	F9 III	0.46:	5.00	110	1100	26	20	22	4.5	7	20	32	59	150	10,11	
μ Vel	G5 III	0.68	3.41	27	380	7.2	9.9	2.2	2.1	2.5	2:	3.7	8.2	80	1,12	
α Aur Aa	G6 III	0.68:	8.18	170	360	9	4.8	1.4:	1.1	0.5:	1.3:	2.1:	4:	...	10,11	
λ And	G8 III-IV+	0.78	2.47	10.6	1600	40	38	13	19	5.2	9.9	27	42	260:	1,6,10	
β Cet	K1 III	0.72	5.03	52	260	6.0	4.5	1.0	1.1	1.9	1.5	1.0	4.4	40	1,12	
ϵ Sco	K2 III-IV	0.86	5.88	48	71	1.4	1.0	<0.1	...	<0.2	...	0.6:	0.8:	0.3	1,4,13	
α Ser	K2 III	0.81	4.49	33	67	1.2	0.9	<0.2	...	<0.4	...	0.6:	1.0:	0.3	1,4,13	
α Boo	K2 III	0.97	20.3	490	95	2.0	0.7	<0.1	<0.3	<0.1	<0.2	<0.2	<0.4	<0.03	1,13	
δ Vol	F8 II	0.55:	1.46	6.4	510	6.8	2.9	0.9	0.6	2	
β Dra	G2 II	0.68	3.27	24	660	26	15	3.9	2.0	3.2	6.7	10	20	30	13,14	
α UMa	K0 II-III+	0.81	6.67	68	100	1.5	0.9:	0.9:	<0.2	1,4,13	
δ CMa	F8 Ia	0.51	3.61	50	62	1.7	...	0.4	0.6:	...	0.6:	<0.3	2,4	
β Aqr	G0 Ib	0.61	2.71	20	260	8	4	0.7	0.6	0.8	1.3	1.5	3.6	<1	12,15	
α Aqr	G2 Ib	0.66	2.94	20	590	15	4.5	1.0	1.0	1.0	1.3	1.6	4.0	<1	12,15	
ϵ Gem	G8 Ib	0.96	5.19	29	280	20	3.1	...	1.1?	0.9?	...	<0.3	<1?	...	13,14	
56 Peg	K0 Ibp	0.97	2.31	5.8	550	40	19	6.7	10	5.5	16	30	52	...	13,16	
λ Vel	K5 Ib	1.24	12.3	100	110	4.8	1.1	...	0.3	13,15	

^aStellar angular diameter (see Linsky *et al.* 1979). Surface fluxes equal apparent fluxes times $(4.125 \times 10^8 / \phi)^2$.

^bREFERENCES.—(1) This work; (2) Böhm-Vitense and Dettmann 1980; (3) Ayres and Linsky 1980a; (4) Vaiana *et al.* 1980; (5) Walter *et al.* 1980b; (6) Basri and Linsky 1979; (7) Johnson 1981; (8) Kondo *et al.* 1976; (9) Simon and Linsky 1980; (10) Walter *et al.* 1980a; (11) Ayres and Linsky 1980b; (12) *Einstein* collaborative guest observation (courtesy G. S. Vaiana); (13) Stencel *et al.* 1980; (14) Basri and Linsky 1981; (15) Hartmann, Dupree, and Raymond 1980; (16) Courtesy R. E. Stencel.

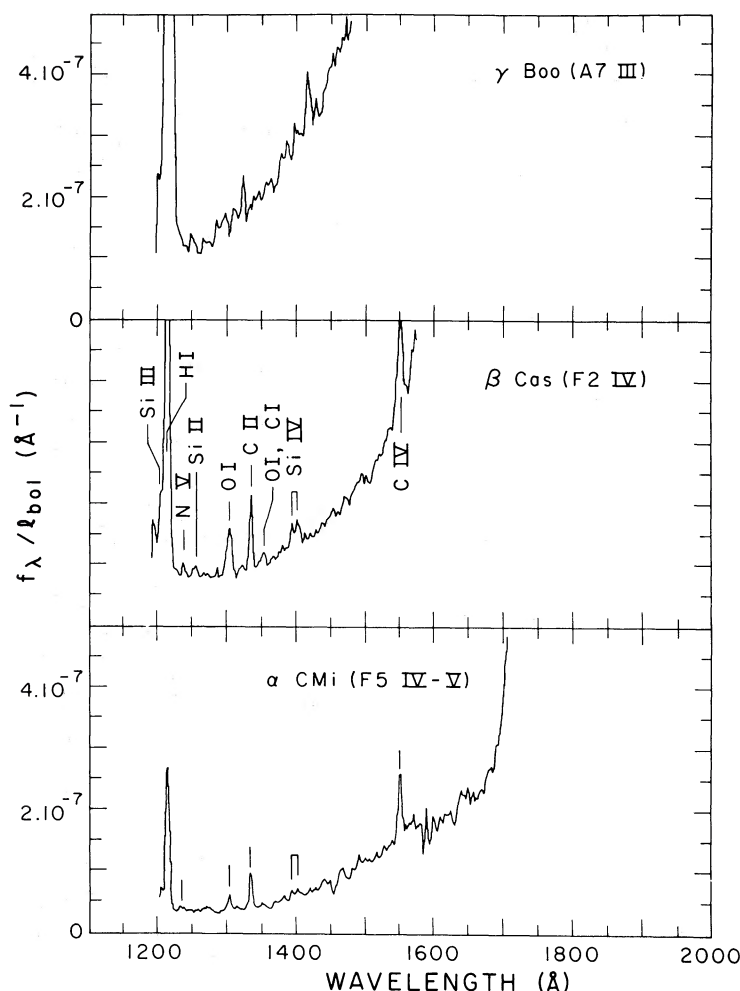


FIG. 1.— Sample IUE spectra of F subgiants and a late-A giant in the 1150–2000 Å short-wavelength region. The ordinate is a flux ratio that represents the monochromatic fraction of the stellar bolometric output at each wavelength (units are \AA^{-1}). As such, the normalized spectra of dwarfs and giants can be compared directly. The background consists of the unresolved photospheric spectrum and some scattered light from longer wavelengths.

to early K, continuing the trend seen in Figure 1. The normalized continuum strength in the longer wavelength portion of this spectral region is a useful guide to cool-star effective temperatures. In fact, the presence of anomalous emission in this spectral band can indicate the presence of previously unrecognized hot-star companions (see, e.g., Mariska, Doschek, and Feldman 1980).

Figure 3 compares the SWP spectra of several G–K giants. We see immediately an enormous diversity of ultraviolet emission line strengths in what is a comparatively small region of the H-R diagram. The two G giants (μ Vel and λ And) and one of the early K giants (β Cet) exhibit prominent transition-region emission lines (N v, Si iv, and C iv), while the remaining K giants (α UMa, ϵ Sco, and α Ser) show little or no evidence for such features.

The weakness, or absence, of hot outer atmospheres in the red giants is illustrated clearly by the archetype K-giant Arcturus (α Boo, K2 III). Figure 4 illustrates a composite spectrum of Arcturus based on a short and long exposure taken through the small aperture. Note that the flux ordinate is magnified by a factor of 25 compared with those of the previous figures. The short exposure of Arcturus was placed on an absolute scale using the integrated fluxes of H I $L\alpha$ and O I $\lambda\lambda 1305, 1356$ measured by a calibrated rocket spectrometer (Weinstein, Moos, and Linsky 1977). The Si II $\lambda\lambda 1808, 1816$ feature was then used as an intermediate standard to transfer the short-exposure calibration to the long exposure.

The Arcturus SWP spectrum is dominated by chromospheric O I emission, although on the ordinate scale

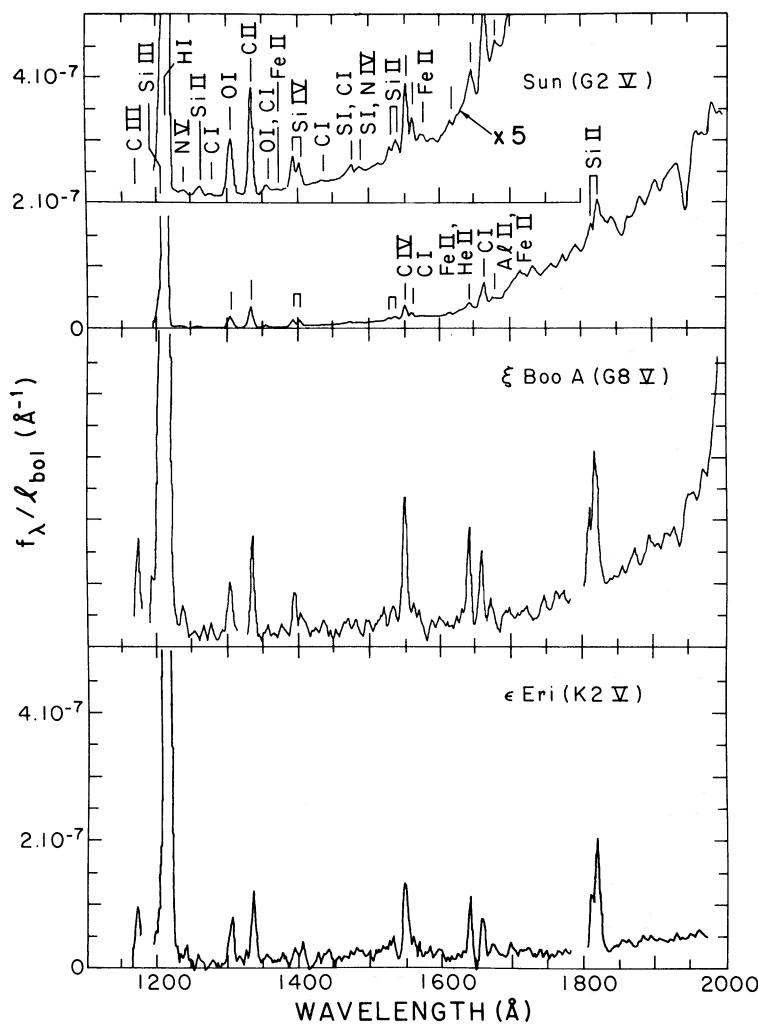


FIG. 2.— Same as Fig. 1 for G-K dwarfs. The solar spectrum depicted here is a moderate-resolution rocket irradiance spectrum that has been smoothed with a Gaussian of 6 Å FWHM to simulate the low-dispersion mode of *IUE*.

of the previous figures the O I feature would be barely noticeable (cf. α Ser and ϵ Sco). At the expanded scale of Figure 4, however, a rich emission-line spectrum appears. Most of the emission structure is attributable to multiplets of Fe II and S I, although several C I and Si II features are apparent. Brown and Jordan (1980*b*) have recently discussed the importance of fluorescence in enhancing the multiplets of neutral sulfur in the red giants. Tentative line identifications in Figure 4 are taken from Brown, Jordan, and Wilson (1979). Despite the rich spectrum, there is no conclusive evidence for high temperature species such as C II λ 1335, Si IV λ 1400, C IV λ 1550, and N V λ 1240. [In fact, weak features that appear near λ 1340 and λ 1550 likely are emission bands of the A-X fourth positive system of carbon monoxide that are fluoresced by O I λ 1305 and C I λ 1657 (Ayres, Moos, and Linsky 1981).] Sensitive echelle-mode ex-

posures are needed to set unambiguous limits on the strength of the hot lines, but rough upper limits can be extracted from the low-dispersion spectra (see below) and are given in Table 2.

In addition to the quantitative line-strength differences between the G and K giant spectra, we note further qualitative distinctions among these stars. In several cases— μ Vel, α UMa, and β Cet—continuum emission in the λ 1800 region appears to be anomalously strong for the assigned MK spectral type. Mu Vel, for example, exhibits considerably brighter continuum emission than expected from a middle G giant, and we suspect that it has an earlier-type dwarf companion or is somewhat earlier in spectral type itself. The same argument can be applied to β Cet, which should show virtually no continuum emission in the λ 1800 region (cf. ϵ Sco and α Ser). Instead, β Cet exhibits appreciable

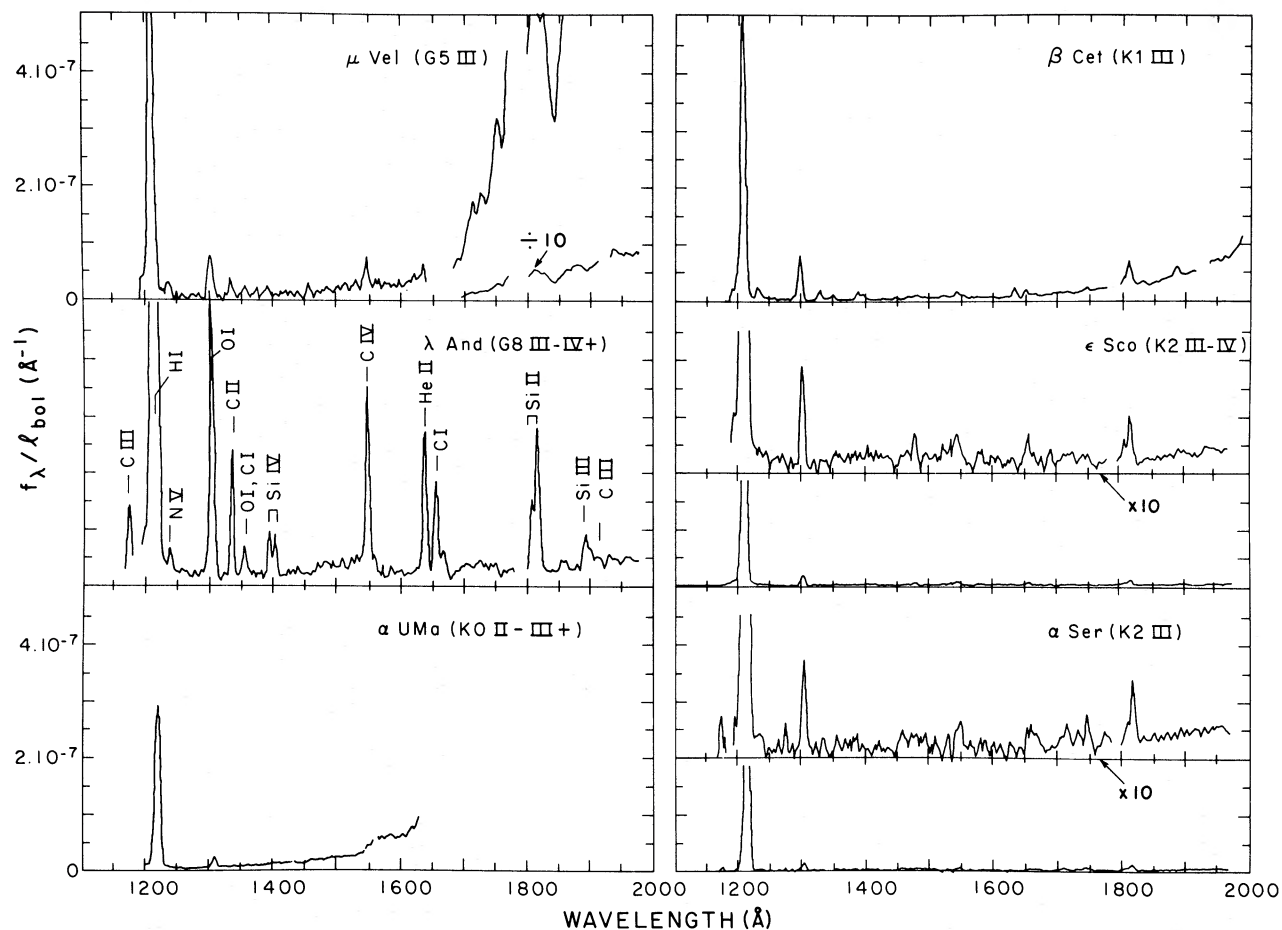


FIG. 3.—Same as Fig. 1 for G-K giants. Note the weakness of the transition-region and chromospheric emission in the K giants compared with the G giants.

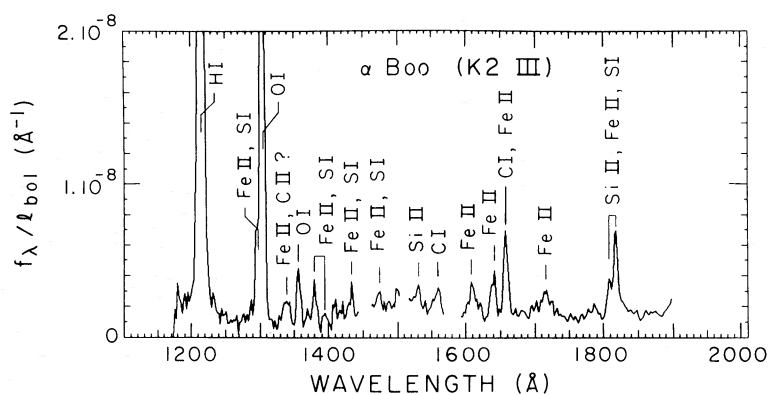


FIG. 4.—Same as Fig. 1 for the K-giant Arcturus. The ordinate scale is magnified a factor of 25 from the previous figures to clarify the rich spectral structure of the short-wavelength region, most of which is attributable to low-excitation chromospheric species. Note also the prominence of the O I triplet blend near $\lambda 1305$, which is thought to be pumped by H I $L\beta$ emission through a Bowen fluorescence mechanism. There is no clear evidence for high-excitation, transition-region species such as Si IV $\lambda 1400$, C IV $\lambda 1550$, or N V $\lambda 1240$. NOTE: the feature at $\lambda 1640$ identified as Fe II is produced mostly by O I + Si I $\lambda 1641$. In addition, several of the emission "lines" may be bands of the CO A-X fourth positive system that are fluoresced by O I $\lambda 1305$ and C I $\lambda 1657$.

emission in that region and is probably a late G, rather than an early K, giant. Finally, α UMa has an extremely bright continuum near $\lambda 1800$ (which saturates the SWP camera even in a short exposure). This anomaly is a consequence of a close, hot companion, likely late-A or early-F in spectral type (Kondo, Morgan, and Modisette 1977).

b) Line Fluxes

In order to establish quantitative relationships among the different stellar spectra, we measured integrated fluxes for the prominent emission features. In practice, we numerically integrated the monochromatic flux above an estimated background level to account for stellar continuum emission and scattered light from longer wavelengths (e.g., Ayres and Linsky 1980*a*, *b*). The resulting line fluxes are summarized in Table 2. Values followed by colons are uncertain, usually because the continuum level is poorly defined. In some cases we estimated flux upper limits from the general "noise" level in the vicinity of the expected position of the target line, and the measured line widths from spectra of other sources where the feature is present. In other cases, we were not able to measure a line flux, or estimate upper limits, owing to saturation of the region of interest. The quiet and active Sun values given in Table 2 are based on the smoothed Mount *et al.* (1980) irradiance spectrum, which was treated in the same manner as the *IUE* stellar spectra, and the active/quiet line ratios cited in that study.

The normalized fluxes (f_l/l_{bol}) in Table 2 measure the fraction of the stellar radiative output emitted by important emission lines from the chromosphere and transition region. Included in the table are stars discussed in this paper as well as data from the literature or otherwise available as noted in the footnotes. (In the latter cases, absence of a line flux entry indicates that a measurement was not provided for the published spectrum.) Seven giants and supergiants in the composite sample have ($V-R$) colors in the range 0.60–0.80. We refer to these stars as yellow giants, and their spectral types extend from G0 Ib (β Aqr) to K1 III (β Cet). These stars have normalized fluxes for the 10^5 K lines (N v, Si IV, and C IV) in the range 4×10^{-7} to 20×10^{-7} , with the exception of the spectroscopic binary λ And (42×10^{-7}). We refer to the giants and supergiants with ($V-R$) > 0.8 as red giants. Six of the seven red giants in Table 2 exhibit normalized fluxes for 10^5 K lines $\leq 1 \times 10^{-7}$. For three of these stars (α Ser, α UMa, and ϵ Sco) the C IV feature is probably real, although the weakness of the emission and possible contamination by fluoresced CO bands precludes a reliable flux determination. For the other three stars (ϵ Gem, α Boo, and λ Vel) only upper limits can be determined; for α Boo the upper limit is $< 0.4 \times 10^{-7}$. Although our data sample is limited, it corroborates the picture originally proposed

by Linsky and Haisch (1979), namely a division occurs in the H-R diagram near ($V-R$) = 0.80 in which the hotter stars (yellow giants) show 10^5 K emission lines with normalized fluxes $\geq 4 \times 10^{-7}$, and the cooler stars (red giants) either show weak 10^5 K emission or upper limits with normalized fluxes $< 1 \times 10^{-7}$.

One of the 14 stars in our sample is clearly exceptional. The star 56 Peg (K0 Ibp, $V-R=0.97$) is a red giant with bright 10^5 K emission ($f_l/l_{\text{bol}} \approx 52 \times 10^{-7}$), as well as variable asymmetry in the Mg II lines. These and other anomalies will be discussed in greater detail by Basri, Stencel, and Linsky (1981).

In addition to our sample, spectra of several other yellow and red giants have been published, although line fluxes are not yet available. For example, Dupree and Hartmann (1980) have presented low-dispersion SWP spectra of five giants ranging in spectral type from G0 III to M0 III. However, aside from the yellow giant β Crv (G5 III, $V-R=0.61$) which exhibits weak C IV emission, these spectra are not sufficiently exposed to determine whether transition-region lines are present or absent. Spectra obtained by Carpenter and Wing (1979) of the yellow giant β Gem (K0 III, $V-R=0.75$) and red giant α TrA (K4 III, $V-R \approx 1.1$) clearly exhibit 10^5 K emission, whereas their spectra of the red giants α Tau (K5 III, $V-R=1.23$) and β And (M0 III, $V-R=1.24$) do not. Finally, Baliunas, Hartmann, and Dupree (1980) state that the Hyades yellow giants 77 Tau (G8 III, $V-R=0.71$) and γ Tau (K0 III, $V-R=0.73$) have bright 10^5 K emission. With the exception of α TrA, these data are consistent with our previous result, namely near ($V-R$) = 0.80 in the H-R diagram a separation occurs between stars that exhibit normalized fluxes in the 10^5 K emission lines $> 4 \times 10^{-7}$ (yellow giants) and $< 1 \times 10^{-7}$ (red giants).

III. EMPIRICAL CORRELATIONS AMONG CHROMOSPHERIC, TRANSITION-REGION, AND CORONAL EMISSIONS

In addition to the emission features of the short-wavelength region, two other diagnostics are useful in comparisons among cool stars: chromospheric Mg II $\lambda 2800$ intensities, and broad-band coronal soft-X-ray fluxes. Since the Mg II *h* and *k* features are important radiative coolants in stellar chromospheres, the doublet emission strength is a useful guide to the overall radiative loss rate of the chromosphere (Linsky and Ayres 1978; Basri and Linsky 1979). Similarly, soft-X-ray fluxes measure coronal radiative losses.

The stellar Mg II fluxes in Table 2 were taken from a variety of sources as noted in the table references. The solar Mg II values are based on *OSO 8* measurements of *h* and *k* in quiet and active regions (courtesy P. Lemaire 1979; see also Chapman 1980). These observations indicate a typical plage/quiet Sun emission contrast of a factor of 5. Sunspot minimum and maximum values of

the Mg II flux were then constructed according to the prescription outlined by Cook, Brueckner, and Van Hoosier (1980)

$$\begin{aligned}\mathcal{F} &= (1-A)\mathcal{F}_Q + A\mathcal{F}_P \\ &= (1-A + A \times R)\mathcal{F}_Q,\end{aligned}\quad (2)$$

where A is the filling factor of plage regions at sunspot maximum (or minimum), \mathcal{F}_Q is the quiet Sun flux, and R is the plage/quiet Sun contrast. In practice, we assumed $A=0.03$ for a typical Zurich sunspot number of $R_Z=40$ at sunspot minimum (Allen 1973), and $A=0.13$ for $R_Z=207$, which corresponds to the moderately active Sun as observed during the Mount *et al.* 1979 June 5 rocket flight. The conversions from R_Z to A are based on the relation proposed by Cook, Brueckner, and Van Hoosier (1980).

The soft-X-ray fluxes tabulated in Table 2 are also from a variety of published and unpublished sources. The bandpass is either 0.1–4.5 keV for the *Einstein* IPC observations or 0.1–3 keV for the *HEAO 1* all-sky survey detections. Several of the stellar soft X-ray measurements are preliminary results of *Einstein* IPC imaging that were kindly made available through a collaborative observing program with the Center for Astrophysics Stellar Survey Team (e.g., Vaiana *et al.* 1980). The quiet and active solar X-ray levels were estimated from the sunspot minimum and maximum fluxes summarized by Manson (1977).

We consider the active/quiet Sun estimates of Mg II fluxes to be reliable, but the broad-band soft-X-ray estimates are considerably less certain. We further note that the stellar Mg II emission strengths may contain systematic errors of up to 20%, owing to the uncertain calibration of the *IUE* LWR camera in the echelle mode (see, e.g., Stencel *et al.* 1980).⁵ However, such uncertainties are not significant in the comparisons described below (particularly because the scales of Mg II temporal variability in cool stars have not yet been established).

Figure 5 compares the normalized emission strengths of prominent chromospheric and transition-region emission lines, and broad-band soft-X-ray fluxes, as functions of normalized Mg II fluxes. The stars are segregated crudely according to spectral type and luminosity class.

The upper left-hand panel of Figure 5 compares the O I resonance triplet ($\lambda\lambda 1302, 1305, 1306$ blend) with

Mg II. We find that the O I emission is well correlated with Mg II, and that the slope of a power-law fit is roughly unity. However, the giant stars tend to have systematically larger O I fluxes at a given Mg II flux level than do the dwarf stars. We conclude that O I is a genuinely “chromospheric” diagnostic (see also Skelton and Shine 1980), but that the mean chromospheric density, which is smaller in giants than in dwarfs (cf. Kelch *et al.* 1978), plays an important role in setting the overall strength of the oxygen emission. This conclusion is plausible because the O I resonance lines are thought to be pumped by H I $L\beta$ through a Bowen-fluorescence mechanism (Bowen 1947), and the pumping should increase substantially with decreasing chromospheric density (Haisch *et al.* 1977).

The upper middle panel compares the Si II triplet ($\lambda\lambda 1808, 1816, 1817$) with Mg II. Here we find a tight, luminosity-independent correlation between the two chromospheric features, although the overall emission levels in Si II are a factor of ≈ 30 smaller. The Si II–Mg II power-law slope of roughly unity would be steepened somewhat if the low-dispersion Si II fluxes of the cooler giant stars (e.g., α Ser and α Boo) are contaminated by significant S I emission as indicated in a high-dispersion observation of the K5 giant α Tau (Brown and Jordan 1980*b*). In fact, Brown and Jordan propose that the S I features near the Si II triplet are pumped by the O I resonance lines, which in turn are pumped by $L\beta$. A Si II slope greater than unity would imply that the Si II lines are formed partly in the transition region (TR) since the pure-TR lines, such as C II and C IV, exhibit power laws steeper than unity (see below). However, a slope near unity is consistent with the calculations by Simon, Kelch, and Linsky (1980) which suggest that the Si II features are formed entirely in the chromosphere.

The top right-hand panel compares the C II resonance doublet ($\lambda\lambda 1335, 1336$ blend) with Mg II. Once again the correlation is strong, at least among the cooler dwarfs and giants, although the slope of the power law appears to be steeper than those of the purely chromospheric O I and Si II features. However, the F stars deviate substantially from the mean trend, in the sense that their C II emission is enhanced relative to Mg II.

The lower left-hand panel compares the He II $\lambda 1640$ $B\alpha$ line and Mg II. Again one finds an excellent correlation, but with an even steeper power-law slope than that for C II. If collisionally excited, He II would be formed at only somewhat hotter levels of the TR than C II. However, photoionization of He⁺ by coronal radiation fields, and subsequent radiative recombinations, are thought to play an important role in producing the $\lambda 1640$ emission (Zirin 1975; Avrett, Vernazza, and Linsky 1976). Accordingly, Hartmann, Dupree, and Raymond (1980) suggest that the He II intensity is a proxy tracer of the coronal soft X-ray emission, and they propose a scaling relation, $f_X \approx 50 f_{\text{He II}}$ (see also

⁵We have adopted a calibration factor of 5.7×10^{-14} ergs $\text{cm}^{-2} \text{s}^{-1} \text{\AA}^{-1}$ (FN per min)⁻¹ at the Mg II lines for converting the standard ripple-corrected spectrum to absolute flux units. The calibration factor is based on the work of Cassatella, Ponz, and Selvelli (1980) and is used by Stencel *et al.* (1980) in an extensive survey of Mg II emission from cool stars. Basri and Linsky (1979) previously adopted 6.8×10^{-14} , and somewhat different calibration factors have been proposed by other authors.

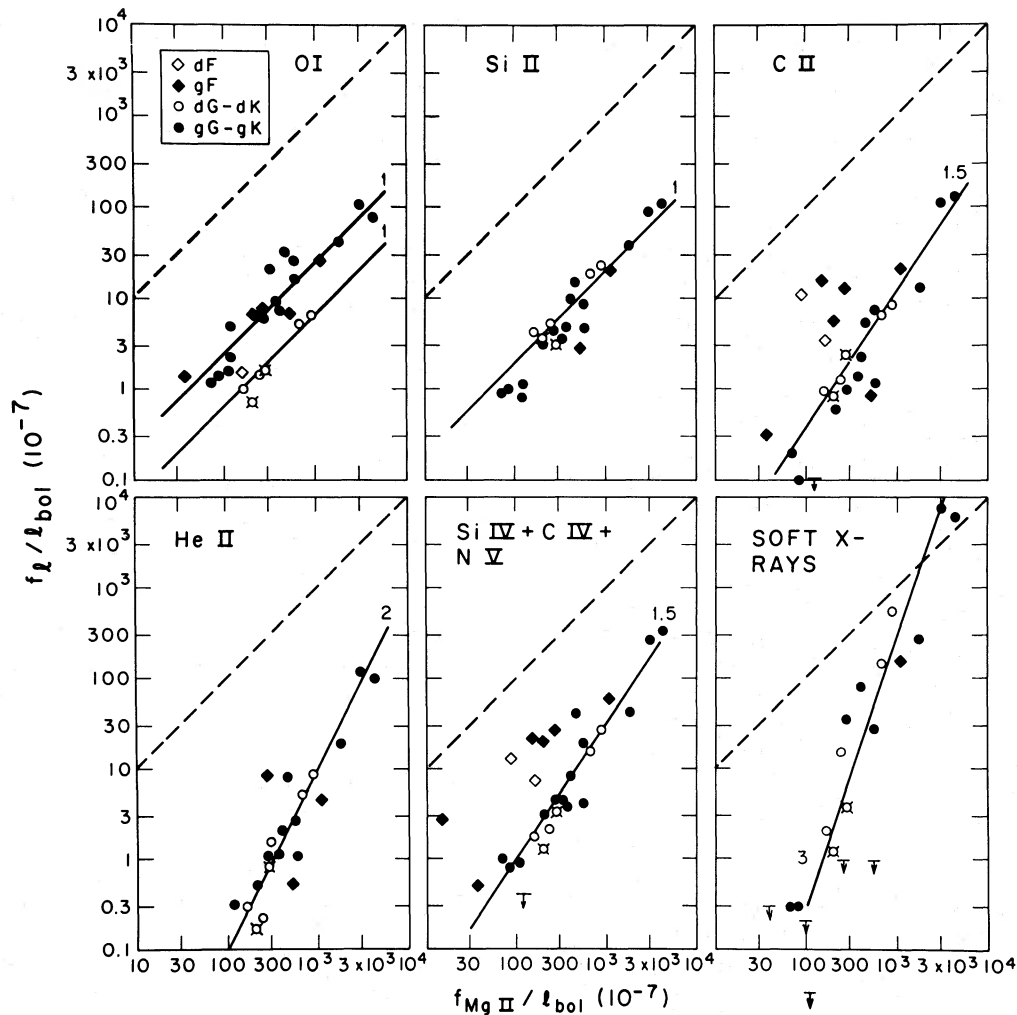


FIG. 5.—Correlations among chromospheric, transition-region, and coronal emissions for F–K dwarfs and giants. The stars have been segregated crudely into four temperature–luminosity classes according to the figure legend. The lines in each panel indicate power laws (with numerical values for the slopes given) that roughly represent the apparent correlations. Values for the Sun at sunspot minimum and maximum are indicated as spiked circles. The dashed line in each panel represents $f_l/l_{\text{bol}} = f_{\text{Mg II}}/l_{\text{bol}}$.

Hartmann *et al.* 1979). Some support for their suggestion is found in the steep power-law slope of the He II–Mg II correlation (but see below).

The middle, bottom panel compares the summed fluxes of Si IV (1400 Å), C IV (1550 Å), and N V (1240 Å) with Mg II. The three TR features are formed over a temperature range of $0.6\text{--}2 \times 10^5$ K, and the sum is usually dominated by C IV. We find a very similar behavior to that of C II; the cooler stars exhibit a tight correlation between the 10^5 K line flux and Mg II with a power-law slope of roughly 1.5, while the F stars deviate systematically from the mean trend. Furthermore, even in the most active stars of the sample (the RS CVn systems HR 1099 and UX Ari), the summed TR fluxes are at least an order of magnitude smaller than the corresponding Mg II fluxes.

The bottom, right panel in Figure 5 compares coronal soft-X-ray emission with Mg II. Again, a rough corre-

spondence of increasing X-ray flux with increasing Mg II flux is apparent, although the power-law slope is steeper than any of the previous comparisons. However, several of the stars for which only upper limits are available (G–K supergiants and late-K giants) fall well below the mean trend, based on G–K dwarfs and F–G giants. For example, the lowest upper limit refers to Arcturus (K2 III). That upper limit should be compared with the detections of the K2 giants α Ser and ϵ Sco (the filled circles immediately below the “3”) at normalized flux levels an order of magnitude larger, despite their slightly smaller Mg II flux ratios. It is probably not coincidental that the giants which were not detected in soft X-rays all show evidence for strong stellar winds and circumstellar envelopes.

Finally, we call attention to the two RS CVn systems (HR 1099 and UX Ari) for which the soft X-ray flux levels exceed the corresponding Mg II fluxes.

IV. DISCUSSION

a) *Summary Implications*

We comment here on the apparent correlations among chromospheric, transition-region coronal emissions illustrated in Figure 5.

1. In the majority of cool stars, the strength of TR and coronal emission is well correlated with the strength of the stellar chromosphere as measured by $f_{\text{Mg II}}/I_{\text{bol}}$. However, some stars, the F dwarfs and giants and certain K giants, for example, seem to deviate significantly from the mean trends. The former tend to exhibit brighter TRs for a given $f_{\text{Mg II}}/I_{\text{bol}}$ ratio, while the latter appear to be deficient in 10^5 K and hotter material. For the stars that exhibit a tight correlation between TR or coronal emission, on the one hand, and chromospheric emission, on the other, the power-law slopes of the relations are steeper than unity. Since the composite Si IV + C IV + N V flux and the soft-X-ray emission level are indicative of the total radiative cooling rates of the 10^5 K layers of the TR and the multimillion degree corona, respectively, we conclude that the *heating* of the extreme outer atmosphere likely has a different functional dependence on stellar parameters than does the heating of the chromosphere itself. One interpretation is that the heating mechanisms are somewhat different in the thermally distinct atmospheric layers, although the very existence of the correlations argues that coronae and chromospheres are *physically* associated. (Such a physical association is well established in the particularly well-studied case of the Sun [e.g., Withbroe and Noyes 1977].)

2. The enhancement of O I emission in the giant stars compared with dwarf stars of similar $f_{\text{Mg II}}/I_{\text{bol}}$ ratios introduces a selection effect in surveys of ultraviolet emission in cool giants obtained with instruments such as *IUE* that have a limited dynamic range. Images that are optimally exposed at the brightest feature of the SWP region aside from L α , namely O I λ 1305, will be underexposed at the C II and C IV lines in cool giants but not in cool dwarfs, if both stars have comparable $f_{\text{Mg II}}/I_{\text{bol}}$ ratios and both follow the TR-Mg II correlation. Given this selection effect and preliminary survey material, it is easy to conclude that transition regions disappear abruptly in the K giant region but not in the K dwarfs, as reported by Linsky and Haisch (1979).

3. Despite the O I selection effect, the weakness or absence of transition-region emission in the red giants ($V-R > 0.80$) noted by Linsky and Haisch is genuine, and the chromospheres of these stars are weak as well. For example, the yellow giants μ Vel and β Cet have chromospheric $f_{\text{Mg II}}/I_{\text{bol}}$ ratios some 3–5 times those of the red giants α UMa, ϵ Sco, α Ser, and α Boo. On the basis of the C II and TR correlation plots in Figure 5, which have power-law slopes of roughly 1.5, one would expect C II/O I or C IV/O I ratios some 5–10 times larger in the yellow giants compared with the red giants.

It is important to recognize that the substantial decline in TR emission levels occurs over a comparatively small change in the broad-band photometric color ($V-R$). For example, the ($V-R$) colors of μ Vel and β Cet are close to 0.70 (0.68 and 0.72, respectively), while those of α UMa, ϵ Sco, and α Ser are ≈ 0.83 (0.81, 0.86, and 0.81, respectively), and that of α Boo is 0.98. The ($V-R$) color is well correlated with effective temperature among such stars (Barnes and Evans 1976), consequently the apparent “sharp” division between strong and weak TR stars in ($V-R$) corresponds to a sharp division in a $L_{\text{bol}}-T_{\text{eff}}$ H-R diagram. Note, however, that an analogous H-R diagram, expressed in terms of M_V spectral type (e.g., Dupree and Hartmann 1980), should exhibit a more diffuse dividing line owing to the only rough correspondence of MK spectral types with effective temperature. For example, β Cet has a bluer ($V-R$) color than is typical of early K giants (0.72 versus 0.81; see, e.g., Johnson 1966) and probably has an effective temperature more typical of a late-G giant.

Clearly, additional data are needed to establish how universal the apparent TR dividing line might be. In particular, the two identified anomalous stars, 56 Peg and α TrA, should be investigated in more detail. Nevertheless, the appearance of even a gross division in the H-R diagram between weak and strong TR giants is a clear signal that some fundamental property of stars or their evolution has a profound influence on the occurrence of hot outer atmospheres.

4. A division in the H-R diagram appears in soft X-rays as well. This is expected given the intimate connection between the TR layers and the corona that is evident in the solar outer atmosphere (Withbroe and Noyes 1977). We do not know at this time what role, if any, circumstellar absorption may play in hiding X-ray emission from the K giants (see below). Nevertheless, the soft-X-ray emission from the detected G–K giants and dwarfs appears to follow an even steeper dependence on the $f_{\text{Mg II}}/I_{\text{bol}}$ ratio than the composite hot-line flux.

5. In the most active stars of our sample, the RS CVn systems UX Ari and HR 1099, the soft-X-ray cooling rate of the stellar corona exceeds the Si IV + C IV + N V cooling of the TR by a factor of 50 or so, whereas for the quiet, solar-type dwarfs the coronal and TR cooling rates are more nearly comparable. This behavior places constraints on models that treat the TR purely as an interface, between the hot corona and the warm chromosphere, that is heated solely by the large flux of heat conducted along the steep temperature gradient separating the two distinct atmospheric layers. If the conductive flux is degraded wholly into radiative emission within the TR, we conclude that heat conduction could be an important cooling source in the coronae of solar-like stars, but it must be relatively *unimportant* in the most active objects.

Indeed, in the UX Ari and HR 1099 systems, the

coronal emission is larger than even the chromospheric Mg II radiative losses, whereas in the solar-like dwarf stars, the chromospheric emission exceeds that of the corona by nearly two orders of magnitude.

6. Finally, the He II soft-X-ray scaling relation proposed by Hartmann, Dupree, and Raymond (1980) apparently is incompatible with the measured flux levels, except perhaps for the brightest of the coronal sources. For example, Hartmann, Dupree, and Raymond (1980) predicted that α Aqr (G2 Ib) would have a soft-X-ray flux in the 1/4 keV band on the order of 7×10^{-12} ergs $\text{cm}^{-2} \text{s}^{-1}$ at the Earth, based on the measured He II flux of 2×10^{-13} . However, the 3σ upper limit for the 0.1–4.5 keV *Einstein* IPC band is only 2×10^{-13} ergs $\text{cm}^{-2} \text{s}^{-1}$. A comparable disparity is found for β Aqr (G0 Ib). There are at least two ways of reconciling the apparent inconsistency.

First, circumstellar material in the α Aqr and β Aqr systems may strongly attenuate any coronal soft-X-ray emission that may be present. In fact, both supergiants exhibit strong violet-shifted absorption features in the Mg II *h* and *k* emission cores (Hartmann, Dupree, and Raymond 1980; Stencel *et al.* 1980) that indicate circumstellar shells and, by implication, strong chromospheric winds. By comparison, β Dra (G2 II) exhibits symmetric Mg II cores (Basri and Linsky 1979, 1981), indicating little or no circumstellar material, and was detected as an *Einstein* source at normalized flux levels a factor of 30 larger than the α Aqr or β Aqr upper limits. A similar comparison can be made between α Boo (K2 III), which has asymmetric Mg II lines and was not detected in X-rays, and α Ser (K2 III), which has comparatively symmetric Mg II lines and is a coronal X-ray source (although weak). Despite the appeal of the circumstellar absorption hypothesis, the solar soft-X-ray emission is only 4–7 times as bright as He II (at *IUE* resolution), consequently an additional mechanism is needed to explain the solar discrepancy.

A second possibility is that the $\lambda 1640$ feature is not purely He II emission in the stars with weak coronae. The solar $\lambda 1640$ feature at 6 Å resolution is a blend of He II, Fe II, S I, and O I (Cohen, Feldman, and Doschek 1978; Kohl 1977; Brown and Jordan 1980*b*; Hartmann *et al.* 1979). Consequently, the intrinsically steep He II–Mg II correlation predicted by the Hartmann *et al.* prescription (namely $f_{\text{He II}} \approx 0.02 f_X \sim f_{\text{Mg II}}^3$) may be diluted significantly by a $f_{\text{Fe II}} \sim f_{\text{Mg II}}^1$ contribution at moderate and low $f_{\text{Mg II}}/I_{\text{bol}}$ levels. [Note: the Fe II component is at least 30% of the total “He II” emission in the Sun (Kohl 1977).] The composite relation might then resemble the empirical He II–Mg II slope of ≈ 2 .

In any event, the possibility that either mechanism—circumstellar obscuration or “Fe II” contamination—is important suggests caution in the practical application of He II soft-X-ray scaling prescriptions to low-dispersion *IUE* spectra.

b) The Importance of Magnetic Fields

The existence of correlations among chromospheric, TR, and coronal emission strengths implies that the different atmospheric layers are physically associated by a unifying mechanism. An obvious candidate for such a mechanism is the magnetic field, as suggested by detailed studies of the Sun over the past decade (Withbroe and Noyes 1977; Vaiana and Rosner 1978). For example, the *Skylab* S-054 synoptic X-ray images of the Sun revealed quite dramatically that the bulk of the bright coronal emission originates in closed magnetic loop structures (Golub *et al.* 1980). Furthermore, the magnetic field plays an equally important role in the physical structure of the solar chromosphere. In particular, Leighton (1959) and Skumanich, Smythe, and Frazier (1975) have established a close connection between mean surface magnetic field strength and solar chromospheric brightness, as measured by the Ca II $\lambda 3934$ K line intensity. The correlation of chromospheric brightness with the surface field strength extends up into the TR, since the morphological peculiarities of the chromosphere—the supergranulation network and plage regions, for example—are seen comparatively unchanged in TR emission lines (e.g., Withbroe 1977). Finally, there is circumstantial evidence that magnetic fields are at the heart of stellar chromospheric and coronal activity. A number of studies have pointed out that chromospheric activity appears to increase with increasing stellar rotational velocity (Wilson 1966; Kraft 1967; Skumanich 1972), particularly in short-period binary systems which contain rapid, synchronous rotators (cf. Bopp and Fekel 1977). A striking example of the rotation-activity connection is the long-period RS CVn-type system Capella (α Aur A; G6 III + F9 III): most of the 10^5 K emission arises from the rapidly rotating F-type secondary, rather than from the optically more luminous but slowly rotating G-type primary (Ayres and Linsky 1980*b*). The rotation-activity connection is compelling circumstantial evidence for the importance of magnetic fields, because *dynamo* action is thought to be a major field regeneration mechanism in rotating, convective stars (e.g., Parker 1970), and dynamo processes should be more vigorous in rapidly rotating stars than in slow rotators.

c) Implications for Chromospheric and Coronal Heating Mechanisms

Athay and White (1978, 1979) and Bruner (1978) have argued, based on high-resolution velocity studies of solar C IV emission with *OSO 8*, that the maximum acoustic wave flux passing through the 10^5 K level of the TR is at least an order of magnitude too small to balance the radiative losses of the overlying TR and coronal layers. Consequently, it is unlikely that the solar outer atmosphere is heated by the deposition of pure acoustic wave energy. Linsky and Ayres (1978) and

Basri and Linsky (1979) have presented evidence that the apparent radiative cooling of stellar chromospheres in general is not compatible with conventional acoustic heating models (e.g., Ulmschneider *et al.* 1977). An alternative mechanism for heating the corona is local field dissipation, for example, by reconnection (see Vaiana and Rosner 1978; Stein and Leibacher 1980). Given the close correspondence of chromospheric Ca II brightnesses with mean magnetic field strength (see above), one might suppose that the chromosphere is also heated by a magnetic field dissipation process. Since the thermal energy density of the coronal plasma is smaller than the magnetic energy density, even for fields of only a few gauss, the dissipation of a small amount of field can replace the coronal energy losses due to radiation and conduction. However, the thermal energy content of the chromospheric plasma is more nearly comparable to the magnetic energy density. Consequently, rather large amounts of magnetic flux must be thermalized on short time scales to replace the local chromospheric heat losses. While such a process may well occur during solar flares, it is not an appealing candidate to explain the quasi-steady heating of the chromospheric layers.

A more plausible possibility is that the small-scale magnetic flux tubes thought to comprise the major component of the solar surface field (e.g., Zwaan 1978) serve as *conduits* of wave energy (acoustic or Alfvén) into the outer atmosphere, or perhaps the presence of the magnetic flux tubes in the subsurface convection zone enhances the local production of acoustic waves (e.g., Stein and Leibacher 1980). Consequently, while magnetic fields very likely provide the *structure* of stellar chromospheres, they may be responsible only indirectly for the *heating*. In any event, the explicit role of the magnetic field in heating stellar chromospheres will likely be revealed only through detailed studies of our own Sun.

d) A Speculative Scenario to Explain the Corona-Wind Boundary in the K-Giant Region

One of the unexpected results from *IUE* observations of cool stars is the absence or weakness of transition regions in the K-giant branch. Because most of the gross structure that appears in the H-R diagram is intimately related to systematic properties of stellar evolution, it is reasonable to ask whether the TR boundary is itself a result of evolutionary effects.

Stellar space-density statistics show that the K giants are a populous stellar type, while G giants are rare by comparison (Allen 1973). There are in fact about as many K giants as A-type main-sequence stars. Since the giant stage occupies only a small fraction of a typical star's lifetime (Iben 1967), the K giants must have evolved from zero age main-sequence (ZAMS) progenitors less massive than the A stars ($\mathcal{M} < 3 \mathcal{M}_{\odot}$). How-

ever, most of the K giants must have been at least as massive as $\sim 1 \mathcal{M}_{\odot}$ on the ZAMS, otherwise they could not have evolved into the giant branch on time scales less than the age of our galaxy ($\approx 10^{10}$ yr). Therefore, the progenitors of the K giants very likely were F or early-G stars on the ZAMS. Similarly, the less numerous G giants very likely were late-B or early-A stars on the ZAMS.

On the one hand, the K giants tend to be old ($t > 3 \times 10^9$ yr), low-mass ($\mathcal{M} \sim 1 \mathcal{M}_{\odot}$) stars that have evolved perpendicularly to contours of constant radius in the H-R diagram from slowly rotating progenitors (F and G dwarfs typically are slow rotators compared with earlier type stars; Kraft 1967). On the other hand, the G giants tend to be young ($t \lesssim 3 \times 10^8$ yr), massive ($\mathcal{M} \gtrsim 3 \mathcal{M}_{\odot}$) stars that have evolved more nearly along isoradius contours from rapidly rotating progenitors. As a result of their substantial evolutionary expansion and slow-rotating antecedents, the old K giants invariably are slow rotators themselves. However, the young G giants, with their more modest evolutionary expansion and rapidly rotating antecedents, very likely are fast rotators. Consequently, the red giants likely have comparatively weak hydromagnetic dynamos and correspondingly weak magnetic/coronal activity, whereas the yellow giants likely have comparatively vigorous dynamos with correspondingly active outer atmospheres.

As a consequence of stellar evolution, therefore, a small region of the giant branch is populated with at least two distinct classes of stars. Owing to the very different evolutionary histories of these two classes (a property not explicitly indicated in the H-R diagram), it is not surprising that the yellow and red giants have qualitatively different outer atmospheres. Note, however, that if chromospheres and coronae were a product of the conventional acoustic wave mechanism (Ulmschneider 1979), one might expect qualitatively similar outer atmospheres in the yellow and red giants, since L_{bol} and T_{eff} , which are similar in the two groups of stars, together establish the initial acoustic flux and the photospheric damping losses, which in turn determine the chromospheric heating (Ulmschneider *et al.* 1977; Linsky 1980).

There is an additional complexity in determining the evolution of a star from its location on the giant branch. Following helium flash at the top of the red giant branch, a massive star returns to the yellow giant region where it remains for a nonnegligible fraction of its lifetime in the helium core burning phase. Although helium flash itself is a much less disruptive episode for $3 \mathcal{M}_{\odot}$ stars than for $1 \mathcal{M}_{\odot}$ stars, potentially significant mass loss could occur that might directly affect the angular momentum of the star (Iben 1965). Such a phenomenon may explain the rotational peculiarities of the Capella giants, namely the slow-rotating primary has probably already suffered helium flash, while the fast-

rotating secondary is likely on its first ascent of the giant branch (Iben 1965).

Another factor that must be considered is the onset of the strong "chromospheric" winds in essentially the same region of the H-R diagram where chromospheres and coronae weaken (e.g., Stencel and Mullan 1980). It is possible, for example, that the winds are fed by a large fraction of the mechanical energy flux that would otherwise heat a hot outer atmosphere (Haisch, Linsky, and Basri 1980). It is also possible that the strength of the wind is independent of the magnetic properties that likely are responsible for the overall chromospheric activity of the star. A "corona-wind" boundary might then result from a secondary influence. For example, the drain of angular momentum by the strong stellar wind would rapidly decrease the rotational velocity already reduced by evolution, and thereby effectively quench the dynamo. Without continual replenishment of the surface magnetic fields, the corona, and perhaps also the chromosphere, would soon fade away. The latter possibility is probably more plausible than the first, since the presence of a strong chromospheric wind is not in itself sufficient to inhibit transition-region (and perhaps also coronal) emission: In the so-called hybrid-spectrum G-supergiants α Aqr and β Aqr, for example, 10^5 K lines

and cool winds appear to coexist (Hartmann, Dupree, and Raymond 1980).

Nevertheless, at this point we cannot decide unambiguously between the two very different alternatives, and the list of alternatives is by no means exhausted (see, e.g., Hartmann and MacGregor 1980). We note that stars to the right of the boundary tend to have lower surface gravities than the stars to the left (which are both more massive and smaller), and surface gravity must certainly play a central role in determining whether a star has a strong or weak wind (e.g., Hartmann and MacGregor 1980). In any event, we have presented a preliminary survey of a complex picture that will become clear only after much additional work. In particular, high-resolution spectroscopy is needed to determine unambiguously the contribution of weak, high-temperature features in a crowded spectrum such as that of Arcturus.

This work was supported in part by National Aeronautics and Space Administration grants NAG5-82 and NGL-06-003-057 through the University of Colorado. We wish to thank Dr. A. Boggess and the staff of the IUE Observatory for their assistance in the acquisition and reduction of these data.

REFERENCES

- Allen, C. W. 1973, *Astrophysical Quantities*, 3d ed. (London: Athlone).
- Athay, R. G., and White, O. R. 1978, *Ap. J.*, **226**, 1135.
- _____. 1979, *Ap. J. Suppl.*, **39**, 333.
- Avrett, E. H., Vernazza, J. E., and Linsky, J. L. 1976, *Ap. J. (Letters)*, **207**, L199.
- Ayres, T. R., and Linsky, J. L. 1980a, *Ap. J.*, **235**, 76.
- _____. 1980b, *Ap. J.*, **241**, 279.
- Ayres, T. R., Linsky, J. L., Garmire, G., and Córdova, F. 1979, *Ap. J. (Letters)*, **232**, L117.
- Ayres, T. R., Moos, H. W., and Linsky, J. L. 1981, submitted.
- Baliunas, S. L., Hartmann, L., and Dupree, A. K. 1980, in *The Universe at Ultraviolet Wavelengths: The Second Year of IUE*, ed. R. Chapman (NASA Spec. Report), in press.
- Barnes, T. G., and Evans, D. S. 1976, *M.N.R.A.S.*, **174**, 489.
- Basri, G. S., and Linsky, J. L. 1979, *Ap. J.*, **234**, 1023.
- _____. 1981, *Ap. J.*, **247**, in press.
- Basri, G. S., Stencel, R. E., and Linsky, J. L. 1981, in preparation.
- Boggess, A. et al. 1978, *Nature*, **275**, 372.
- Bohlin, R. C., Holm, A. V., Savage, B. D., Sniijders, M. A. J., and Sparks, W. M. 1980, *Astr. Ap.*, **85**, 1.
- Böhm-Vitense, E., and Dettmann, T. 1980, *Ap. J.*, **236**, 560.
- Bopp, B. W., and Fekel, F., Jr. 1977, *A. J.*, **82**, 490.
- Bowen, I. S. 1947, *Pub. A.S.P.*, **59**, 196.
- Brown, A., and Jordan, C. 1980a, *Proceedings of The Second European IUE Conference (ESA SP-157)*, in press.
- _____. 1980b, *M.N.R.A.S.*, **191**, 37P.
- Brown, A., Jordan, C., and Wilson, R. 1979, *The First Year of IUE*, ed. A. J. Willis (London: University College), p. 232.
- Bruner, E. C., Jr. 1978, *Ap. J.*, **226**, 1140.
- Carpenter, K. G., and Wing, R. F. 1979, *Bull. AAS*, **11**, 419.
- Cash, W., Bowyer, S., Charles, P., Lampton, M., Garmire, G., and Riegler, G. 1978, *Ap. J. (Letters)*, **223**, L21.
- Cash, W., Charles, P., Bowyer, S., Walter, F., Ayres, T. R., and Linsky, J. L. 1979, *Ap. J. (Letters)*, **231**, L137.
- Cash, W., and Snow, T. P., Jr. 1980, preprint.
- Cash, W., Snow, T. P., Jr., and Charles, P. 1979, *Ap. J. (Letters)*, **232**, L111.
- Cassatella, A., Holm, A., Ponz, D., and Schiffer, F. H. 1980, *NASA IUE Newsletter*, No. 8, p. 1.
- Cassatella, A., Ponz, D., and Selvelli, P. L. 1980, preprint.
- Cohen, L., Feldman, U., and Doschek, G. A. 1978, *Ap. J. Suppl.*, **37**, 393.
- Cook, J. W., Brueckner, G. E., and Van Hoosier, M. E. 1980, *J. Geophys. Res.*, **85**, 2257.
- Dupree, A. K. 1975, *Ap. J. (Letters)*, **200**, L27.
- Dupree, A. K., and Hartmann, L. 1980, in *Stellar Turbulence*, eds. D. F. Gray and J. L. Linsky (New York: Springer-Verlag), p. 279.
- Flannery, B. P., and Ayres, T. R. 1978, *Ap. J.*, **221**, 175.
- Fröhlich, C. 1977, in *The Solar Output and Its Variation*, ed. O. R. White (Boulder: Colorado Associated University Press), p. 93.
- Golub, L., Maxson, C., Rosner, R., Serio, S., and Vaiana, G. S. 1980, *Ap. J.*, **238**, 343.
- Haisch, B. M., Linsky, J. L., and Basri, G. S. 1980, *Ap. J.*, **235**, 519.
- Haisch, B. M., Linsky, J. L., Weinstein, A., and Shine, R. A. 1977, *Ap. J.*, **214**, 785.
- Hartmann, L., Davis, R., Dupree, A. K., Raymond, J., Schmidtke, P. C., and Wing, R. F. 1979, *Ap. J. (Letters)*, **233**, L69.
- Hartmann, L., Dupree, A. K., and Raymond, J. C. 1980, *Ap. J. (Letters)*, **236**, L143.
- Hartmann, L., and MacGregor, K. B. 1980, *Ap. J.*, **242**, 260.
- Holm, A. 1979, *NASA IUE Newsletter*, No. 7, p. 27.
- Iben, I., Jr. 1965, *Ap. J.*, **142**, 1447.
- _____. 1967, *Ann. Rev. Astr. Ap.*, **5**, 571.
- Johnson, H. L. 1966, *Ann. Rev. Astr. Ap.*, **4**, 193.
- Johnson, H. L., Mitchell, R. I., Iriarte, B., and Wisniewski, W. Z. 1966, *Comm. Lunar Planet. Lab.*, **4**, 99.
- Johnson, H. M. 1981, *Ap. J.*, **243**, 234.
- Kelch, W. L., Linsky, J. L., Basri, G. S., Chiu, H. Y., Chang, S., Maran, S. P., and Furenliid, I. 1978, *Ap. J.*, **220**, 962.
- Kohl, J. H. 1977, *Ap. J.*, **211**, 958.
- Kondo, Y., Duval, J. E., Modisette, J. L., and Morgan, T. H. 1976, *Ap. J.*, **210**, 713.
- Kondo, Y., Morgan, T. H., and Modisette, J. L. 1976, *Ap. J.*, **207**, 167.
- _____. 1977, *Pub. A.S.P.*, **89**, 163.
- Kraft, R. P. 1967, *Ap. J.*, **150**, 551.
- Leighton, R. B. 1959, *Ap. J.*, **130**, 366.
- Lemaire, P. 1979, private communication.

- Linsky, J. L. 1980, *Ann. Rev. Astr. Ap.*, **18**, 439.
 Linsky, J. L., and Ayres, T. R. 1978, *Ap. J.*, **220**, 619.
 Linsky, J. L., and Haisch, B. M. 1979, *Ap. J. (Letters)*, **229**, L27.
 Linsky, J. L., and Marstad, N. C. 1980, in *The Universe at Ultraviolet Wavelengths: The Second Year of IUE*, ed. R. Chapman (NASA Spec. Rept.), in press.
 Linsky, J. L. *et al.* 1978, *Nature*, **275**, 389.
 Linsky, J. L., Worden, S. P., McClintock, W., and Robertson, R. M. 1979, *Ap. J. Suppl.*, **41**, 47.
 Manson, J. E. 1977, in *The Solar Output and Its Variation*, ed. O. R. White (Boulder: Colorado Associated University Press), p. 261.
 Mariska, J. T., Doschek, G. A., and Feldman, U. 1980, *Ap. J. (Letters)*, **238**, L87.
 Mewe, R., Heise, J., Gronenschild, E. H. B. M., Brinkman, A. C., Schrijver, J., and den Boggende, A. J. F. 1975, *Ap. J. (Letters)*, **202**, L67.
 Mount, G. H., Rottman, G. J., and Timothy, J. G. 1980, *J. Geophys. Res.*, **85**, 4271.
 Nugent, J., and Garmire, G. 1978, *Ap. J. (Letters)*, **226**, L83.
 Parker, E. N. 1970, *Ann. Rev. Astr. Ap.*, **8**, 1.
 Simon, T., Kelch, W. L., and Linsky, J. L. 1980, *Ap. J.*, **237**, 72.
 Simon, T., and Linsky, J. L. 1980, *Ap. J.*, **241**, 759.
 Skelton, D., and Shine, R. A. 1980, preprint.
 Skumanich, A. 1972, *Ap. J.*, **171**, 565.
 Skumanich, A., Smythe, C., and Frazier, E. N. 1975, *Ap. J.*, **200**, 747.
 Stein, R. F., and Leibacher, J. 1980, in *Stellar Turbulence*, ed. D. F. Gray and J. L. Linsky (New York: Springer), p. 225.
 Stencel, R. E., and Mullan, D. J. 1980, *Ap. J.*, **238**, 221.
 Stencel, R. E., Mullan, D. J., Linsky, J. L., Basri, G. S., and Worden, S. P. 1980, *Ap. J. Suppl.*, **44**, 383.
 Topka, K., Fabricant, D., Harnden, F. R., Jr., Gorenstein, P., and Rosner, R. 1979, *Ap. J.*, **229**, 661.
 Ulmschneider, P. 1979, *Space Sci. Rev.*, **24**, 71.
 Ulmschneider, P., Schmitz, F., Renzini, A., Cacciari, C., Kalkofen, W., and Kurucz, R. L. 1977, *Astr. Ap.*, **61**, 515.
 Vaiana, G. S., and Rosner, R. 1978, *Ann. Rev. Astr. Ap.*, **16**, 393.
 Vaiana, G. S. *et al.* 1980, *Ap. J.*, **245**, 163.
 Vitz, R. C., Weiser, H., Moos, H. W., Weinstein, A., and Warden, E. S. 1976, *Ap. J. (Letters)*, **205**, L35.
 Walter, F. M., Cash, W., Charles, P. A., and Bowyer, C. S. 1980a, *Ap. J.*, **236**, 212.
 Walter, F. M., Charles, P. A., and Bowyer, C. S. 1978, *A.J.*, **83**, 1539.
 Walter, F. M., Linsky, J. L., Bowyer, C. S., and Garmire, G. 1980b, *Ap. J. (Letters)*, **236**, L137.
 Weinstein, A., Moos, H. W., and Linsky, J. L. 1977, *Ap. J.*, **218**, 195.
 Wilson, O. C. 1966, *Ap. J.*, **144**, 695.
 Withbroe, G. L. 1977, in *Proceedings of the OSO-8 Workshop* (Boulder: Colorado Associated University Press), p. 2.
 Withbroe, G. L., and Noyes, R. W. 1977, *Ann. Rev. Astr. Ap.*, **15**, 363.
 Zirin, H. 1975, *Ap. J. (Letters)*, **199**, L63.
 Zwaan, C. 1978, *Solar Phys.*, **60**, 213.

THOMAS R. AYRES: Laboratory for Atmospheric and Space Physics, University of Colorado, Boulder, CO 80309

JEFFREY L. LINSKY and NORMAN C. MARSTAD: Joint Institute for Laboratory Astrophysics, University of Colorado, Boulder, CO 80309